Medicinal Chemistry Research (2020) 29:1507–1519
https://doi.org/10.1007/s00044-020-02577-6

MEDICINAL CHEMISTRY RESEARCH

ORIGINAL RESEARCH

Synthesis, evaluation of cytotoxicity, and antimicrobial activity of A-azepano- and A-seco-3-amino-C28-aminolupanes

Oxana B. Kazakova[1] · Tatyana V. Lopatina[1] · Irina P. Baikova[1] · Zulfia R. Zileeva[2] · Yulia V. Vakhitova[2] · Kyrill Yu. Suponitsky[3,4]

Received: 16 March 2020 / Accepted: 27 May 2020 / Published online: 7 June 2020

Abstract

A series of new C28-amino-lupanes bearing A-azepano- and A-seco-3-amino-fragments was synthesized from 3,28-dioximino-betulin and evaluated for cytotoxicity toward the NCI-60 cancer cell line panel and antimicrobial activity against key ESKAPE pathogens. A-azepano-28-amino-betulin exhibited remarkable activities with GI_{50} ranging from 1.16 to 2.27 μM against all panel with the highest activity toward leukemia, colon cancer, non-small cell lung cancer and breast cancer. The replacement of the hydroxyl group at C28 in the structure of azepanobetulin to the amino group did not show a strong effect on the cytotoxic activity. Both compounds were ~5 and ~4 times more active than doxorubicin against colon cancer HCT-15 and ovarian cancer NCI/ADR-RES cell lines, thus these A-azepano-lupane triterpenoids are the promising agents for future anticancer drug development. The ability of A-azepanobetulin to inhibit cell growth may be associated with its cytostatic effect, which, depending on the cell line, is associated with the arrest either S or G1 phase of cell cycle. 3-Amino-3,4-seco-28-amino-lup-4(23),20(29)-dien exhibited significant bacteriostatic effect against methicillin-resistant *Staphylococcus aureus* (MIC ≤ 0.25 μg/mL) that exceeds the effect of the clinically used antibiotic vancomycin.

Graphical Abstract

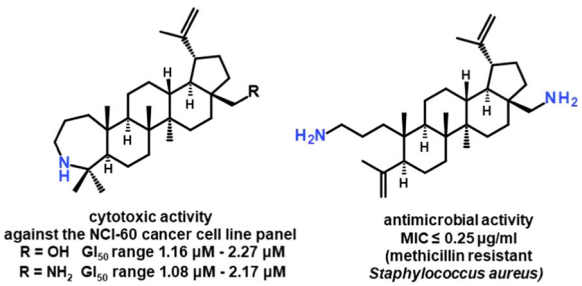

Keywords Triterpenoids · Lupane · Betulin · Beckmann rearrangement · Lactame · Azepane · Cytotoxicity · Antimicrobial activity

Supplementary information The online version of this article (https://doi.org/10.1007/s00044-020-02577-6) contains supplementary material, which is available to authorized users.

✉ Oxana B. Kazakova
obf@anrb.ru

[1] Ufa Institute of Chemistry UFRC RAS, 71 pr. Oktyabrya, Ufa, Russian Federation450054

[2] Institute of Biochemistry and Genetics UFRC RAS, 71 pr. Oktyabrya, Ufa, Russian Federation450054

[3] A.N. Nesmeyanov Institute of Organoelement Compounds, Russian Academy of Sciences, Moscow, Russian Federation119991

[4] Plekhanov Russian University of Economics, Stremyanny per. 36, Moscow, Russian Federation117997

Introduction

Lupane type triterpenoids (lupeol, betulin, betulinic, and betulonic acids) are widespread in the plant kingdom including the bark of birch trees and display important biological properties such as anticancer, antiviral, antibacterial, and antimalarial activities, among others (Tolstikov et al. 2005; Tolstikova et al. 2006; Krasutsky 2006; Csuk 2014; Sousa et al. 2019; Bildziukevich et al. 2019). In particular, the antitumor properties of lupanes have attracted considerable attention worldwide since many synthetic derivatives of these triterpenoids have shown promising results as chemotherapeutic agents for different types of cancer (Csuk 2014; Zhang et al. 2015; Ali-Seyed et al. 2016; Sousa et al. 2019; Bildziukevich et al. 2019). Recently, pentacyclic triterpenoids were identified as antimicrobial and antibiofilm agents, and as adjuvants in restoring the activity of common antibiotics against *Staphylococcus aureus* (Chung 2019; Catteau et al. 2018). Since bacteria are the most common pathogens causing infections in oncologic patients (Hoz et al. 2019), the search of agents combining both anticancer and antimicrobial activities is actual.

Over the past years, a large number of lupane triterpenoids have been chemically modified in order to improve their bioactivity and bioavailability and to enhance their protective and/or therapeutic effects. Among these derivatives, triterpenoids with A-azepane ring are a group of new and promising modificants with anticancer (Kazakova et al. 2014; Lopatina et al. 2019; Giniyatullina et al. 2019; Smirnova et al. 2019), antimicrobial (Medvedeva et al. 2018; Kazakova et al. 2019a, b) and alpha-glucosidase inhibitory (Khusnutdinova et al. 2016) activities. Based on the results we obtained with A-azepanes of lupane, oleanane, ursane, and dammarane types, the recent investigation has been focused on the synthesis of A-azepano- and A-seco-3-amino-lupanes with C28-amino-substituent as well as A-azepano-lupeol, and evaluation of their cytotoxicity with cell cycle analysis and antimicrobial activity.

Experimental

General

The spectra were recorded at the Center for the Collective Use "Chemistry" of the Ufa Institute of Chemistry of the UFRC RAS and RCCU "Agidel" of the UFRC RAS. X-ray diffraction experiments were carried out using the equipment of Center for molecular composition studies of INEOS RAS. ^{1}H and ^{13}C-NMR spectra were recorded on a "Bruker AM-500" (Bruker, Billerica, MA, USA, 500 and 125.5 MHz, respectively, δ, ppm, Hz) in $CDCl_3$, internal standard tetramethylsilane. Mass spectra were obtained on a liquid chromatograph–mass spectrometer LCMS-2010 EV (Shimadzu, Kyoto, Japan). Single crystal X-ray diffraction study was carried out with SMART APEX II CCD diffractometer (λ(Mo-Kα) = 0.71073 A, graphite monochromator, ω-scans) at 120 K. Collected data were processed by the SAINT and SADABS programs incorporated into the APEX2 program package (Bruker 2014). The structures were solved by the direct methods and refined by the full-matrix least-squares procedure in anisotropic approximation for non-hydrogen atoms (Sheldrick 2015). Melting points were detected on a micro table "Rapido PHMK05" (Nagema, Dresden, Germany). Optical rotations were measured on a polarimeter "Perkin-Elmer 241 MC" (Perkin-Elmer, Waltham, MA, USA) in a tube length of 1 dm. Elemental analysis was performed on a Euro EA-3000 CHNS analyzer (Eurovector, Milan, Italy); the main standard is acetanilide. Thin-layer chromatography analyses were performed on Sorbfil plates (Sorbpolimer, Krasnodar, Russian Federation), using the solvent system chloroform–ethyl acetate, 40:1. Substances were detected by 10% H_2SO_4 with subsequent heating to 100–120 °C for 2–3 min. Betulin dioxime **1** (Flekhter et al. 2002), compounds **2** (Khusnutdinova et al. 2019), **3** (Tolmacheva et al. 2018), and **10** (Lopatina et al. 2019) were obtained according to the methods described previously.

Chemistry

Crystallographic data for compound (2)

$C_{30}H_{46}N_2O$ are monoclinic, space group $P2_1$: $a = 6.6272$ (7) Å, $b = 27.629(3)$ Å, $c = 14.252(2)$ Å, $\beta = 90.409(3)°$, $V = 2609.5(5)$ Å^3, $Z = 4$, $M = 450.69$, $d_{cryst} = 1.147$ g cm^{-3}. $wR^2 = 0.1259$ calculated on F^2_{hkl} for all 11,545 independent reflections with $2\theta < 27.1°$, (GOF = 0.955, $R = 0.0656$ calculated on Fhkl for 6124 reflections with $I > 2\sigma(I)$). Crystallographic data (excluding structure factors) for the structure have been deposited at the Cambridge Crystallographic Data Centre (CCDC) as supplementary publication No. CCDC 1986798.

Synthesis of compounds (4) and (6)

To a solution of 1 mmol of compound **2** or **3** in anhydrous THF (40 mL) 2.2 mmol (0.08 g) of $LiAlH_4$ was added and a mixture was refluxed for 1 h, then poured into 5% HCl (100 mL), the product was extracted with $CHCl_3$, chromatographed on a column with Al_2O_3, eluting with $CHCl_3$ and a mixture of $CHCl_3$—EtOH (100:1, 50:1).

3-deoxy-3a-homo-3a-aza-28-amino-lup-20(29)-en (4)

Yield 0.36 g (82%); the spectral and physicochemical data are in agreement with those from the literature (Kazakova et al. 2019b).

3-amino-3,4-seco-28-amino-lup-4(23),20(29)-dien (6)

Yield 0.34 g (77%); MP 121 °C; $[\alpha]_D^{20} + 163°$ (c 0.05, $CHCl_3$); δ_H (500.13 MHz, $CDCl_3$) 0.85, 0.98, 1.21, 1.33, 1.68 (5 s, 15H, $5CH_3$), 1.72–2.42 (m, 25H, CH and CH_2), 2.60 and 3.00 (both d, $^2J = 12.9$ Hz, 2H, H-28), 3.01–3.13 (m, 4H, H-3, H-2), 3.36 (br. s, 2H, NH_2), 4.64 and 4.66 (both d, $^2J = 1.8$ Hz, 2H, H-24), 4.69 and 4.78 (both d, $^2J = 2.0$ Hz, 2H, H-29); δ_C (125.76 MHz, $CDCl_3$) 14.75, 16.05, 19.12, 19.40, 20.51, 21.41, 26.85, 27.28, 29.22, 29.40, 32.01, 33.40, 34.26, 37.58, 38.79, 39.26, 40.18, 40.83, 42.74 (C-3), 43.16, 47.83, 48.77 (C28), 49.48, 50.43, 51.26, 56.60, 109.71 (C-29), 112.86 (C-24), 148.28 (C-4), 150.52 (C-20); Anal. Calcd for $C_{30}H_{52}N_2$: C, 81.75; H, 11.89; N, 6.36. Found: C, 81.71; H, 11.87; N, 6.32.

3-oxo-3a-homo-3a-aza-28-amino-lup-20(29)-en (5)

To a solution of 1 mmol (0.45 g) of compound **2** in anhydrous THF (20 mL), 2.2 mmol (0.08 g) of $LiAlH_4$ was added and a mixture was stirred at room temperature for 1 h, then poured into 5% HCl (50 mL), the products were extracted with $CHCl_3$ and chromatographed on a column with Al_2O_3, eluting with $CHCl_3$ and a mixture of $CHCl_3$—EtOH (150:1, 100:1, 50:1). Yield 0.035 g (8%) of compound **4**, 0.12 g (27%) of compound **5**, and recovery of compound **2** 0.26 g (58%). For compound **5** MP 145 °C; $[\alpha]_D^{20} + 127$ (c 0.05, $CHCl_3$); δ_H (500.13 MHz, $CDCl_3$) 0.83, 1.03, 1.05, 1.20, 1.28, 1.62 (6 s, 18H, $6CH_3$), 1.70–2.58 (m, 25H, CH and CH_2), 2.62 and 3.03 (both d, $^2J = 12.9$ Hz, 2H, H-28), 3.33 (br. s, 2H, NH_2), 4.56 and 4.71 (both d, $^2J = 2.0$ Hz, 2H, H-29), 5.59 (br. s, 1H, NH); δ_C (125.76 MHz, $CDCl_3$) 14.63, 15.94, 18.26, 19.21, 21.92, 22.51, 25.41, 26.85, 27.28, 29.22, 29.40, 32.01, 33.40, 34.26, 37.54, 38.81, 39.26, 40.20, 40.88, 42.74, 46.09, 47.02 (C-28), 47.06, 48.98, 50.78, 53.00, 56.26, 110.22 (C-29), 149.52 (C-20), 176.31 (C-3); Anal. Calcd for $C_{30}H_{50}N_2O$: C, 79.24; H, 11.08; N, 6.16. Found: C, 80.19; H, 11.84; N, 6.20.

Synthesis of compounds (7–9)

A rapid stream of ozone was passed through a solution of compound **2** or **3** or **4** (1 mmol) in CH_2Cl_2 (30 mL) at −40 °C until the starting compound disappeared (TLC control). The solvent was removed under reduced pressure, and the residue was purified by column chromatography on Al_2O_3 eluting with $CHCl_3$ and a mixture of $CHCl_3$—EtOH (100:1, 50:1) giving compound **7** or **8** or **9**.

3-oxo-3a-homo-3-aza-20-oxo-17-nitrilo-29-nor-lupane (7)

Yield 0.40 g (88%); MP 195 °C; $[\alpha]_D^{20} + 21°$ (c 0.05, $CHCl_3$); δ_H (500.13 MHz, $CDCl_3$) 0.88, 1.01, 1.04, 1.24, 1.29 (5 s, 15H, $5CH_3$), 1.40–2.10 (m, 19H, CH and CH_2), 2.12 (s, 3H, H-30), 2.23–2.90 (m, 6H, CH and CH_2), 5.81 (br. s, 1H, NH); δ_C (125.76 MHz, $CDCl_3$) 14.56, 15.72, 18.20, 21.64, 22.43, 27.21, 27.36, 27.46, 28.89, 30.19, 30.42, 31.98, 33.27, 33.55, 35.74, 39.33, 40.20, 40.28, 40.58, 42.38, 48.84, 49.01, 50.61, 51.63, 52.86, 56.17, 122.05 (C28), 176.26 (C-3), 209.78 (C-20); Anal. Calcd for $C_{29}H_{44}N_2O_2$: C, 76.95; H, 9.80; N, 6.16. Found: C, 77.00; H, 9.84; N, 6.12.

3,4-seco-4,20-dioxo-2,17-dinitrilo-23,29-dinorlupane (8)

Yield 0.32 g (74%); MP 81 °C; $[\alpha]_D^{20}$ −66° (c 0.05, $CHCl_3$); δ_H (500.13 MHz, $CDCl_3$) 0.91, 0.93, 1.11, 2.11, 2.18 (5 s, 15H, $5CH_3$), 1.22–2.42 (m, 23H, CH and CH_2), 2.88–2.90 (m, 2H, CH); δ_C (125.76 MHz, $CDCl_3$) 11.50, 14.59, 15.92, 19.48, 20.77, 21.62, 26.53, 27.45, 28.95, 30.13, 30.41, 30.64, 31.83, 34.67, 35.71, 38.95, 39.97, 40.17, 40.33, 42.61, 48.75, 48.91, 51.77, 56.25, 119.83 (C28), 122.75 (C-3), 209.66 (C-4), 211.49 (C-20); Anal. Calcd for $C_{28}H_{40}N_2O_2$: C, 77.02; H, 9.23; N, 6.42. Found: C, 77.69; H, 9.26; N, 6.50.

3-deoxy-3a-homo-3a-aza-20-oxo-28-amino-29-norlupane (9)

Yield 0.34 g (76%); MP 221 °C; $[\alpha]_D^{20} + 73°$ (c 0.05, $CHCl_3$); δ_H (500.13 MHz, $CDCl_3$) 0.85, 0.99, 1.05, 1.17, 1.41 (5 s, 15H, $5CH_3$), 2.15 (s, 3H, H-30), 1.65–2.40 (m, 28H, CH and CH_2), 2.78–2.90 (2H, m, H-28), 3.35–3.29 (1H, m, H-3_a), 3.80–3.78 (1H, m, H-3_b); δ_C (125.76 MHz, $CDCl_3$) 14.51, 16.55, 16.61, 19.15, 21.30, 21.66, 22.08, 22.78, 22.93, 23.08, 25.79, 26.86, 27.77, 28.99, 29.66, 33.96, 37.71, 40.72, 40.91, 41.22, 43.10, 47.45 (C28), 47.61, 47.84, 48.59, 54.74, 60.51, 67.98 (C-3), 211.49 (C-20); Anal. Calcd for $C_{29}H_{50}N_2O$: C, 78.68; H, 11.38; N, 6.33. Found: C, 78.55; H, 11.99; N, 6.40.

3-deoxy-3a-homo-3a-aza-lup-20(29)-en (11) was synthesized according to Kumar et al. (2008). Yield 0.34 g (79%); MP 178 °C; $[\alpha]_D^{20} + 155°$ (c 0.05, $CHCl_3$); Liter. (Kumar et al. 2008) MP 185–188 °C; δ_H (500.13 MHz, $CDCl_3$) 0.78, 0.90, 1.09, 1.15, 1.48, 1.57, 1.68 (7 s, 21H, $7CH_3$), 1.70–2.50 (m, 25H, CH and CH_2), 3.00 (br. s, 1H, NH), 3.30 (br. s, 2H, H-2), 4.50 and 4.70 (both d, $^2J = 2.0$ Hz, 2H, H-29); δ_C (125.76 MHz, $CDCl_3$) 14.29, 16.47, 16.58, 18.07, 19.35, 21.33, 21.51, 22.85, 23.05, 25.74, 27.27, 27.83, 29.78, 33.64, 35.40, 38.39, 39.47, 39.95,

40.77, 41.09, 41.17, 43.04, 43.10, 47.37, 47.76, 48.32, 54.39, 63.15, 109.49 (C-29), 150.73 (C-20); Anal. Calcd for $C_{30}H_{51}N$: C, 84.64; H, 12.07; N, 3.29. Found: C, 84.70; H, 12.00; N, 3.30.

Pharmacological studies

Anticancer assay

In vitro cancer screen in National Cancer Institute (NCI), USA The screening is a two-stage process, beginning with the evaluation of all compounds against the 60 cell lines at a single dose of 10^{-5} M. Compounds that exhibit significant growth inhibition are evaluated against the 60 cell panel at five concentration levels. The human tumor cell lines of the cancer-screening panel are grown in RPMI 1640 medium containing 5% fetal bovine serum and 2 mM *L*-glutamine. For a typical screening experiment, cells are inoculated into 96-well microtiter plates in 100 mL at plating densities ranging from 5000 to 40,000 cells/well depending on the doubling time of individual cell lines. After cell inoculation, the microtiter plates are incubated at 37 °C, 5% CO, 95% air, and 100% relative humidity for 24 h prior to addition of experimental drugs. After 24 h, two plates of each cell line are fixed in situ with TCA, to represent a measurement of the cell population for each cell line at the time of drug addition (time zero (Tz)). Experimental drugs are solubilized in dimethylsulfoxide at 400-fold the desired final maximum test concentration and stored frozen prior to use. At the time of drug addition, an aliquot of frozen concentrate is dissolved and diluted to twice the desired final maximum test concentration with complete medium containing 50 mg/mL gentamicin. Additional four, 10-fold or ½ log serial dilutions are made to provide a total of five drug concentrations plus control. Aliquots of 100 mL of these different drug dilutions are added to the appropriate microtiter wells already containing 100 mL of medium, resulting in the required final drug concentrations. Following drug addition, the plates are incubated for an additional 48 h at 37 °C, 5% CO, 95% air, and 100% relative humidity. For adherent cells, the assay is terminated by the addition of cold TCA. Cells are fixed in situ by the gentle addition of 50 mL of cold 50% TCA (final concentration, 10% TCA) and incubated for 60 min at 4 °C. The supernatant is discarded, and the plates are washed five times with tap water and air dried. Sulforhodamine B (SRB) solution (100 mL) at 0.4% in 1% acetic acid is added to each well, and plates are incubated for 10 min at room temperature. After staining, the unbound dye is removed by washing five times with 1% acetic acid and the plates are air dried. The bound stain is subsequently solubilized with 10 nm Trizma base, and the absorbance is read on an automated plate reader at a wavelength of 515 nm. For suspension cells, the methodology is the same except that the assay is terminated by fixing settled cells at the bottom of the wells by gently adding 50 mL of 80% TCA (final concentration, 16% TCA). Using the seven absorbance measurements [Tz, control growth (C), and test growth in the presence of drug at the five concentration levels (Ti)], the percentage growth is calculated at each of the drug concentrations levels. Percentage growth inhibition is calculated as:

$[(\text{Ti\_Tz})/(\text{C\_Tz})]\_100$ for concentrations for which Ti_Tz,

$[(\text{Ti\_Tz})/\text{Tz}]\_100$ for concentrations for which Ti < Tz.

Three dose response parameters are calculated for each experimental agent. Growth inhibition of 50% (GI_{50}) is calculated from [(Ti_Tz)/(C_Tz)]_100 ¼ 50, which is the drug concentration resulting in a 50% reduction in the net protein increase (as measured by SRB staining) in control cells during the drug incubation. The drug concentration resulting in total growth inhibition (TGI) is calculated from (Ti ¼ Tz). The LC_{50} (concentration of drug resulting in a 50% reduction in the measured protein at the end of the drug treatment as compared with that at the beginning) indicating a net loss of cells following treatment is calculated from:

$[(\text{Ti\_Tz})/\text{Tz}]\_100^{1}/_{4}\_50.$

Values are calculated for each of these three parameters if the level of activity is reached; however, if the effect is not reached or is exceeded, the value for that parameter is expressed as greater or less than the maximum or minimum concentration tested (Boyd and Paul 1995; Grever et al. 1992; Monks et al. 1991, 1997; Weinstein et al. 1997).

Cell cycle analysis HEK293 (2×10^3 cells/well), SH-SY5Y (2.5×10^5 cells/well), A549 (5×10^4 cells/well) cells were seeded in 24-wells plates and cultured for 24 h followed by treatment with compound **10** for 72 h (at IC_{50} values previously determined for distinct cell line). Cells of control group were treated with 0.1% DMSO. Cells were harvested and fixed in 70% ice-cold ethanol overnight. Subsequently, the cells were centrifuged, the supernatant was discarded and the pellet was treated with RNase A (50 µg/mL) for 5 min at room temperature. The treated cells were stained with propidium iodide (50 µg/mL) for 15 min at room temperature in the dark. The cells were then analyzed for cell cycle distribution by flow cytometry ("Novocyte® 2060," "ACEA Bioscience Inc," USA) and the changes in the cell cycle profiles were analyzed using "NovoExpress 1.2.5" ("ACEA Bioscience Inc," USA). Experiments were repeated independently two times in triplicate.

Antimicrobial and antifungal assays

Sample preparation Samples were prepared in DMSO and water to a final testing concentration of 32 μg/mL, in 384-well, nonbinding surface plate for each bacterial/fungal strain and keeping the final DMSO concentration to a maximum of 1% DMSO. All the sample preparations were done using liquid handling robots. Compounds that showed solubility issues during stock solution preparation are detailed in the datasheet.

Antimicrobial assay

Procedure All bacteria were cultured in cation-adjusted Mueller–Hinton broth at 37 °C overnight. A sample of each culture was then diluted 40-fold in fresh broth and incubated at 37 °C for 1.5–3 h. The resultant mid-log phase cultures were diluted (CFU/ml measured by OD_{600}), then added to each well of the compound-containing plates, giving a cell density of 5×10^5 CFU/mL and a total volume of 50 μl. All the plates were covered and incubated at 37 °C for 18 h without shaking.

Analysis Inhibition of bacterial growth was determined measuring absorbance at 600 nm (OD_{600}), using a Tecan M1000 Pro monochromator plate reader. The percentage of growth inhibition was calculated for each well, using the negative control (media only) and positive control (bacteria without inhibitors) on the same plate as references. The significance of the inhibition values was determined by modified *Z*-scores, calculated using the median and MAD of the samples (no controls) on the same plate. Samples with inhibition value above 80% and *Z*-score above 2.5 for either replicate were classed as actives. Samples with inhibition values between 50 and 80% and *Z*-score above 2.5 for either replicate were classed as partial actives.

Hit confirmation The percentage of growth inhibition was calculated for each well, using the negative control (media only) and positive control (bacteria without inhibitors) on the same plate. The MIC was determined as the lowest concentration at which the growth was fully inhibited, defined by an inhibition ≥ 80%. In addition, the maximal percentage of growth inhibition is reported as D_{Max}, indicating any compounds with partial activity. Hits were classified by MIC ≤ 16 μg/mL in either replicate.

Antifungal assay

Procedure Fungi strains were cultured for 3 days on yeast extract-peptone dextrose agar at 30 °C. A yeast suspension of 1×10^6 to 5×10^6 CFU/mL (as determined by OD_{530}) was prepared from five colonies. The suspension was subsequently diluted and added to each well of the compound-containing plates giving a final cell density of fungi suspension of 2.5×10^3CFU/mL and a total volume of 50 μL. All plates were covered and incubated at 35 °C for 24 h without shaking.

Analysis Growth inhibition of *Candida albicans* was determined measuring absorbance at 530 nm (OD_{530}), while the growth inhibition of *Cryptococcus neoformans* was determined measuring the difference in absorbance between 600 and 570 nm ($OD_{600–570}$), after the addition of resazurin (0.001% final concentration) and incubation at 35 °C for additional 2 h. The absorbance was measured using a Biotek Synergy HTX plate reader. The percentage of growth inhibition was calculated for each well, using the negative control (media only) and positive control (fungi without inhibitors) on the same plate. The significance of the inhibition values was determined by modified *Z*-scores, calculated using the median and MAD of the samples (no controls) on the same plate. Samples with inhibition value above 80% and *Z*-score above 2.5 for either replicate ($n = 2$ on different plates) were classed as actives. Samples with inhibition values between 50 and 80% and *Z*-score above 2.5 for either replicate were classed as partial actives.

Hit confirmation In both cases, the percentage of growth inhibition was calculated for each well, using the negative control (media only) and positive control (fungi without inhibitors) on the same plate. The MIC was determined as the lowest concentration at which the growth was fully inhibited, defined by an inhibition ≥ 80% for *C. albicans* and an inhibition ≥ 70% for *C. neoformans*. Due to a higher variance in growth and inhibition, a lower threshold was applied to the data for *C. neoformans*. In addition, the maximal percentage of growth inhibition is reported as D_{Max}, indicating any compounds with marginal activity. Hits were classified by MIC ≤ 16 μg/mL in either replicate.

Antibiotic, cytotoxic, and hemolytic standards preparation and quality control (QC)

Colistin and vancomycin were used as positive bacterial inhibitor standards for gram-negative and gram-positive bacteria, respectively. Fluconazole was used as a positive fungal inhibitor standard for *C. albicans* and *C. neoformans*.

The QC of the assays was determined by Z′-factor, calculated from the negative (media only) and positive controls (bacterial, fungal, or cell culture without inhibitor), and the standards. Plates with a Z′-factor of ≥0.4 and standards active at the highest and inactive at the lowest concentration were accepted for further data analysis.

Results and discussion

Chemistry

3,28-Dioximino-betulin **1** was taken as the starting compound for the designed A-azepano- and A-seco-3-amino-lupanes with C17-CH_2NH_2 substituent. Dioxime **1** is available from the betulonic aldehyde (Flekhter et al. 2002) and possesses promising activities (Yli-Kauhaluoma et al. 2010). The Beckmann rearrangement of dioxime **1** by the treatment with $SOCl_2$ in dioxane according to the previously described method (Medvedeva et al. 2018) led to a mixture A-azepanono-17-nitrile **2** and 3,4-seco-4(23)-en-2,17-dinitrile **3** with yields of 55% and 38%, respectively, after isolation by column chromatography. The spectral and physicochemical data for the obtained compounds **2** and **3** were in agreement with those from the literature (Khusnutdinova et al. 2019; Tolmacheva et al. 2018). Moreover, the X-ray analysis of compound **2** (Fig. 1) confirms the location of lactame system at C3a position and that the nitrogen atom is situated between C-3 and C-4 atoms. Therefore, the C-3-oxime group in compound **1** reveals *E* configuration which is in agreement with those for oleanolic acid lactame (Bednarczyk-Cwynar et al. 2013). The reduction of compound **2** or **3** with $LiAlH_4$ under reflux in THF for 1 h affected both lactame and nitrile-groups with the formation of amines **4** and **6** in good yields. The same reaction provided at room temperature led to a mixture of products with full (compound **4**) and fractional regioselective reduction (compound **5**) and yields of 8% and 27%, respectively, and recovery of initial compound **2** (58%) after purification by column chromatography (Scheme 1). In the ^{13}C-NMR spectra of compounds **4**–**6** the signal of the carbon atom C28 is observed at δ 47.02–47.77 ppm and in the ^{1}H NMR spectra characteristic signals of H-28 protons were appeared as two doublets at δ 2.60–2.62 and 3.00–3.03 ppm, as well as broadened signals of the NH_2 group at δ 3.30–3.36 ppm. The C-3 carbon atom signal for compound **4** is detected at δ 63.2 ppm which is in agreement with those for A-azepanotriterpenoids (Medvedeva et al. 2018), for compound **6** — at δ 42.74 ppm (Giniyatullina et al. 2020). The presence of the lactam cycle in compound **5** was confirmed by the characteristic C-3 carbon signal at δ 176.31 ppm and NH-proton of lactame ring at δ 5.59 ppm.

Ozonolysis of compound **2**, **3**, or **4** led to 20-oxo-29-nor-derivative **7**, **8**, or **9**, respectively. In the ^{13}C-NMR spectra of these compounds C-20(29) double bond signals were not observed but the C-20 signal of the oxo-group appeared at δ 209.78–213.50 ppm. To compare the influence of substituent at C17 on the biological activities of A-azepano-lupanes azepanobetulin **10** and azepano-lupeol **11** were also synthesized as previously described (Lopatina et al. 2019; Kumar et al. 2008).

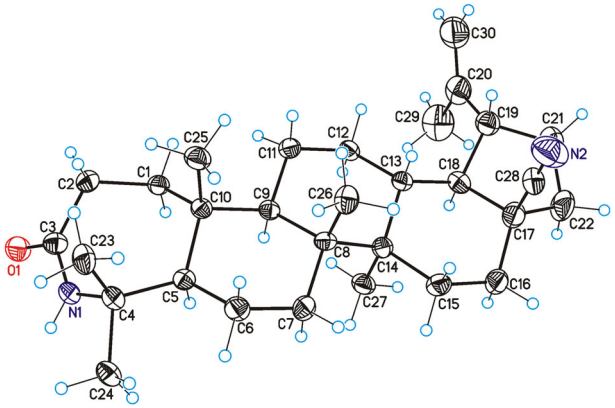

Fig. 1 Thermal ellipsoid plot (50%) and labeling scheme for compound **2**

Biological activity

Evaluation of cytotoxicity activity

The synthesized lupane derivatives **2–11** were evaluated for their in vitro antitumor activity (cytotoxicity) toward 60 cell lines of nine different types of human cancers (lung, colon, central nervous system, ovary, renal, prostate, breast tumors, leukemia, and melanoma) according to the protocols available at the NCI (Bethesda, USA) in a single concentration 10^{-5} M. Each cell line was inoculated and preincubated on a microtiter plate after that test compound was added and the culture was incubated for 48 h. Results were reported as the percent of growth of the treated cells compared with the untreated control cells (negative numbers indicate cell kill). According to the NCI criteria (reduction of the growth of any one of the cancer cell lines to ca. 32% or less), compounds **2**, **3**, and **7** did not show cytotoxic activity against the studied cell lines. Compound **6** was active against leukemia (K-562 and SR) and colon cancer (HT29). Compound **8** inhibited the cell growth of the leukemia cell lines (CCRF-CEM, HL-60(TB), and MOLT-4), CNS cancer (SF-295 and SNB-75) and cell line renal cancer (RXF 393) and breast cancer (HS 578T). Compound **9** showed activity against one colon cancer cell line (HT29), whereas compound **11** was active toward leukemia (K-562, RPMI-8226, SR), colon cancer (COLO 205, HCT-116, HCT-15, HT29, SW-620), CNS cancer (U251), and breast cancer (MDA-MB-468). Compound **5** inhibits leukemia cell lines (CCRF-CEM, HL-60(TB), K-562, MOLT-4, SR), colon cancer (HCT-116, HT29), and melanoma (MALME-3M, UACC-257). Compound **4** showed the greatest antiproliferative activity toward 56 cell lines, resulting in 48 cases of cancer cell lethality from −9.72 to −97.20% (Table 1).

Compound **4**, which exhibited the most promising results in single-dose test and fulfilling the NCI criteria for activity

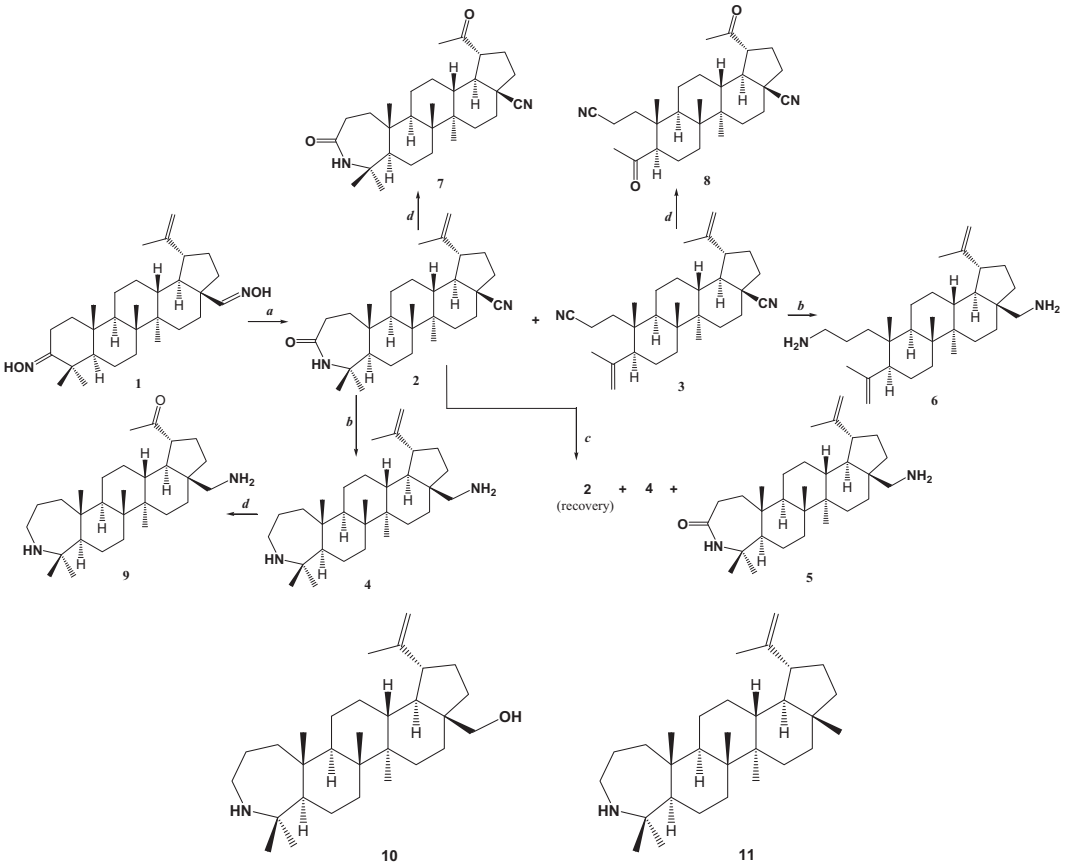

Scheme 1 Reagents and conditions: a $SOCl_2$, 1,4-dioxane; 30 min; b $LiAlH_4$, THF, reflux 1 h; c $LiAlH_4$, THF, 22 °C, 1 h; d O_3, CH_2Cl_2, −40 °C

in that preliminary assay, was further investigated in a five-dose testing mode at ten-fold dilution (100–0.01 μM) over the full panel. For this compound, three response parameters, the GI_{50} (the concentration producing 50% GI, a measure of compound potency), TGI (the concentration producing 100% GI, a measure of compound efficacy), and LC_{50} (the concentration causing 50% lethality, a measure of compound efficacy and cytotoxicity), were determined and are summarized in Table 2.

Compound **4** exhibited remarkable activities with GI_{50} ranging from 1.16 to 2.27 μM against all panels of NCI-60. The highest anticancer activity was observed against leukemia cell lines with the values of GI_{50} 1.16 μM (K-562) and 1.21 μM (SR), colon cancer cell lines with GI_{50} 1.19 μM (HCT-15), non-small cell lung cancer cell line with GI_{50} 1.24 μM (NCI-H460) and breast cancer with GI_{50} 1.27 μM (MCF7). Azepanobetulin **10** was taken for the comparison and exhibited remarkable activities with GI_{50} ranging from 1.08 to 2.17 μM against all panels of NCI-60 (Lopatina et al. 2019) (Table 2).

In general, the replacement of the hydroxyl group by the amino group in compound **4** does not have a strong effect on the cytotoxic activity of these compounds. Pronounced activity against cell lines of leukemia (K-562), colon cancer (HCT-15), and breast cancer (MCF7) remains the same for both compounds **4** and **10**, but cytotoxicity against colon cancer cell lines HCT-116 and HT29 was lower for compound **4** (GI_{50} 1.29 and 1.27 μM for compound **10** and GI_{50} 1.42 and 1.65 μM for compound **4**, respectively), while cytotoxicity against leukemia cell line SR (GI_{50} 1.21 μM for compound **4** instead of GI_{50} 1.59 μM for compound **10**) and non-small cell lung cancer cell line NCI-H460 (GI_{50} 1.24 μM for compound **4** instead of GI_{50} 1.63 μM for compound **10**) was increased (Table 2).

A raw comparison of the activities of compounds **4** and **10** with respect to the activity reported for the standard drug doxorubicin, used by NCI as control (Montoya et al. 2014), reflects that the activity displayed for **4** or **10** was lower than for the standard drug except for cell lines of colon cancer HCT-15 and ovarian cancer NCI/ADR-RES (compounds **4** and **10** were ~5 and ~4 times more active than doxorubicin, respectively). Furthermore, at the LC_{50} level of cytotoxicity, compounds **4** and **10** were more efficient against six cell lines of non-small cell lung cancer, three cell lines of colon cancer, three cell lines of CNS cancer, two cell lines of melanoma, five cell lines of renal cancer, all prostate cancer

Table 1 Percentage cell growth of 60 human tumor cell line anticancer screening data of compounds **2–11** at single-dose assay (10 μM concentration)[a]

Subpanel tumor cell lines	Percentage cell growth for compounds									
	2	3	4	5	6	7	8	9	10[b]	11
Leukemia										
CCRF-CEM	93.34	91.48	**−27.38**	**20.85**	66.63	96.89	**23.45**	93.77	**12.43**	51.97
HL-60(TB)	94.90	70.83	**−52.80**	**−50.48**	53.28	96.07	**29.22**	68.46	**−51.88**	35.74
K-562	78.57	–	**−56.11**	**−4.63**	**1.94**	86.22	48.19	–	**−26.59**	**4.15**
MOLT-4	98.66	68.03	**−45.38**	**21.46**	57.04	91.65	**26.44**	57.93	**4.40**	46.59
RPMI-8226	91.33	82.45	**−43.76**	37.93	58.53	85.21	38.46	89.88	**−36.88**	**30.13**
SR	90.22	79.06	**−38.71**	**−27.13**	**−3.93**	77.53	42.21	64.88	**−40.44**	**1.20**
NSC lung cancer										
A549/ATCC	83.09	86.84	**−68.36**	59.25	82.67	95.10	74.33	94.78	44.88	51.30
EKVX	100.58	79.54	**6.81**	87.25	102.08	84.95	67.76	93.19	63.26	103.22
HOP-62	99.30	98.14	**21.22**	81.58	90.64	99.81	67.62	102.83	78.96	101.12
HOP-92	79.49	83.93	**−29.39**	54.60	67.43	82.17	71.09	81.63	81.99	76.56
NCI-H226	92.04	96.19	53.87	88.06	90.60	93.69	75.74	100.25	84.36	96.49
NCI-H23	95.29	96.44	**10.47**	85.28	91.09	99.22	68.03	89.32	62.57	94.13
NCI-H322M	103.00	95.96	**−42.74**	89.09	90.18	94.08	80.44	93.10	69.84	99.50
NCI-H460	109.77	94.32	**−78.32**	90.33	94.75	99.61	59.78	93.86	**−54.44**	48.37
NCI-H522	68.80	71.97	**−31.01**	88.01	93.97	92.75	61.81	90.39	64.19	105.63
Colon cancer										
COLO 205	91.36	98.67	**−71.21**	75.92	34.49	98.83	103.93	96.63	**−63.45**	**8.77**
HCC-2998	113.18	94.40	**−80.64**	97.73	76.96	98.94	88.57	102.23	**−5.02**	65.97
HCT-116	92.21	70.40	**−95.46**	**11.72**	50.09	92.45	46.23	72.96	**−78.86**	**5.39**
HCT-15	106.97	98.58	**−92.44**	38.73	62.76	94.41	79.92	83.16	**3.28**	**19.19**
HT29	75.48	62.28	**−85.84**	**11.54**	**17.86**	95.92	45.43	**28.25**	**2.58**	**3.37**
KM12	102.33	92.19	**−85.41**	81.02	88.14	98.19	54.88	92.08	**23.20**	66.82
SW-620	111.51	94.89	**−84.54**	75.93	88.86	102.76	90.48	96.17	**−66.45**	**2.47**
CNS cancer										
SF-268	96.30	82.67	**22.86**	64.47	79.87	90.99	60.42	90.88	61.21	104.50
SF-295	96.25	83.61	**−59.62**	82.05	100.78	94.68	**24.61**	95.95	40.41	106.06
SF-539	108.69	89.12	**−31.78**	75.23	90.40	95.37	47.88	91.67	34.26	98.21
SNB-19	94.97	102.12	**−58.51**	78.40	89.52	89.23	57.30	99.85	49.62	96.25
SNB-75	99.11	92.95	**−27.72**	85.47	79.75	87.77	**27.46**	93.19	77.06	85.90
U251	90.87	98.55	**−89.70**	53.41	74.01	89.20	48.63	90.51	**7.49**	**11.85**
Melanoma										
LOX IMVI	98.13	101.43	**−98.28**	–	–	–	57.82	86.11	**−57.73**	–
MALME-3M	105.59	88.93	**−70.52**	**−14.11**	80.18	93.65	77.75	83.71	**−65.40**	88.89
M14	100.28	88.81	**−77.69**	70.92	75.17	89.50	56.75	88.28	**−49.76**	79.55
MDA-MB-435	104.85	93.01	**−96.20**	92.74	96.24	98.77	72.30	94.84	**13.55**	84.59
SK-MEL-2	98.61	69.38	**6.75**	98.81	107.27	105.68	52.74	89.47	78.76	119.45
SK-MEL-28	106.12	98.06	**−28.27**	89.16	100.03	102.56	54.12	103.74	**−65.40**	104.96
SK-MEL-5	96.13	98.20	**−9.72**	61.65	88.28	87.36	41.05	94.06	**−82.49**	98.43
UACC-257	92.97	90.55	46.29	**29.58**	99.73	101.90	79.68	105.73	**−8.72**	106.63
UACC-62	86.10	78.92	**29.03**	82.54	100.22	87.58	46.52	95.85	43.16	104.75
Ovarian cancer										
IGROV1	111.21	91.41	**−81.87**	70.33	86.94	113.68	65.52	87.28	36.30	93.96
OVCAR-3	102.60	88.89	**−85.82**	87.97	89.40	98.12	66.82	95.03	44.42	76.18

Table 1 (continued)

Subpanel tumor cell lines	Percentage cell growth for compounds									
	2	3	4	5	6	7	8	9	10[b]	11
OVCAR-4	96.72	82.91	**−70.91**	70.71	101.55	87.51	–	100.10	**31.81**	94.53
OVCAR-5	110.28	107.70	**−22.98**	97.81	103.14	98.89	104.94	104.11	74.96	107.44
OVCAR-8	95.49	99.58	**−59.61**	66.52	94.06	96.59	71.84	100.91	**23.54**	84.12
NC/ADR-RES	92.94	102.04	**−52.02**	69.97	94.55	98.81	87.73	101.65	44.82	97.31
SK-OV-3	86.51	104.71	86.12	92.02	107.01	104.16	74.30	122.07	92.20	112.80
Renal cancer										
786-0	101.91	84.02	**−97.20**	84.55	81.77	98.95	47.60	98.96	**30.17**	102.44
A498	–	93.61	–	96.23	88.69	88.61	83.38	84.70	–	79.73
ACHN	103.11	99.88	**−91.78**	69.06	99.13	99.95	63.36	102.08	50.20	95.46
CAKI-1	95.83	57.71	**−94.50**	59.88	75.46	69.52	72.14	94.29	38.39	75.31
RXF 393	107.74	92.93	**−87.37**	59.03	79.03	100.00	**15.59**	94.25	48.36	88.40
SN12C	102.13	100.96	**−25.54**	65.64	82.54	91.82	61.31	92.25	45.93	82.14
TK-10	106.34	85.21	**−10.60**	113.85	118.60	107.21	106.15	108.33	80.77	141.88
UO-31	102.36	79.38	**5.31**	58.90	62.97	91.35	54.76	71.02	53.76	88.24
Prostate cancer										
PC-3	80.00	64.60	**−10.50**	37.37	71.49	80.94	42.94	76.10	**25.61**	78.88
DU-145	103.60	93.94	**−53.45**	74.97	94.79	103.16	88.05	98.29	49.53	75.62
Breast cancer										
MCF7	90.77	86.67	**−66.10**	41.52	71.77	80.60	39.53	76.62	**−12.60**	**33.35**
MDA-MB-231/ATCC	100.09	92.54	**−79.66**	58.68	92.76	94.44	62.56	100.08	46.85	96.71
HS 578T	111.33	104.89	**−42.29**	84.12	89.36	72.06	**26.40**	93.96	46.76	100.73
BT-549	109.29	107.79	84.63	80.83	92.12	90.30	56.40	94.50	77.10	101.17
T-47D	79.17	80.14	**−10.12**	53.89	88.57	92.90	52.44	94.30	36.46	75.98
MDA-MB-468	106.21	92.15	**−65.47**	35.49	84.66	95.58	64.93	86.05	**11.74**	**26.16**

[a]Survival of cells cultivated in the presence of 10 μM of the compound under examination (in percent) compared with control cells (without the addition of compound to the culture medium) is given. Negative values correspond to cell death. [b]Lopatina et al. (2019). The symbol "–" designates the absence of data

cell lines, and four breast cancer cell lines. These results suggest that A-azepano-lupanes **4** and **10** are the promising triterpene structures for our future drug development anti-tumor studies.

The mechanism of cell-growth inhibitory activity

In non-cancerous HEK293 cells, A-azepano-betulin **10** causes cell accumulation in the G1 phase, a decrease in the S and G2/M phases and an increase of the apoptotic cells (as evidenced by the appearance of cells in subG1) (Fig. 2). Accordingly, a decrease of HEK293 cell viability upon the action of compound **10** may be due to suppression of proliferation as a result of arrest of the G1 phase. The effect in this case is considered as cytostatic rather than cytotoxic. In SH-SY5Y neuroblastoma cells, compound **10** contributes to a slight increase in the number of cells in the S phase and a decrease in the percentage of cells in phases G1 and G2/M. A decrease in the content of apoptotic cells is statistically significant. In A549 lung carcinoma cells, compound **10** causes an increase in cells in the G1 phase, followed by a decrease in the percentage of cells in the S phase and, more pronounced, in the G2/M phase. The accumulation of apoptotic cells was also noted. The cell cycle arrest in phase G1 testifies in favor of the possible cytostatic action of A-azepanobetulin **10** and suggests the presence of a differentiating effect. Thus, the data on the effect of compound **10** on the cell cycle progression suggest that the suppression of cell growth is mainly governed by the cytostatic effect, which, depending on the cell line, is associated with the arrest either S or G1 phase.

Evaluation of antimicrobial activity

The lupane triterpenoids **2**, **3**, **5**, **6**, and **10** were evaluated at the University of Queensland (Australia) against key

Table 2 In vitro cytotoxic effects of compounds **4** and **10**[c] and standard drug doxorubicin against NCI's human tumor cell line screen

Panel/cell line	4		10[c]		Doxorubicin	
	GI_{50}[a] (μM)	LC_{50}[b] (μM)	GI_{50} (μM)	LC_{50} (μM)	GI_{50} (μM)	LC_{50} (μM)
Leukemia						
CCRF-CEM	2.27	>100	2.07	>100	0.08	100
K-562	1.16	–	1.08	>100	0.19	100
MOLT-4	1.93	>100	1.79[6]	>100	0.03	100
RPMI-8226	1.95	–	1.94	>100	0.08	100
SR	1.21	–	1.59	–	0.03	100
Non-small cell lung cancer						
A549/ATCC	1.95	7.07	1.73	6.06	0.06	100
EKVX	1.77	6.47	1.55	5.92	0.41	47.97
HOP-62	1.93	7.20	1.81	6.46	0.07	67.61
HOP-92	1.69	6.37	1.73	6.42	0.10	42.27
NCI-H226	1.88	100	1.98	843	0.05	6.40
NCI-H23	1.70	6.42	1.71	6.68	0.15	13.15
NCI-H322M	1.61	6.14	1.63	5.64	–	–
NCI-H460	1.24	5.75	1.63	6.30	0.02	51.29
NCI-H522	1.84	–	1.65	–	0.03	2.80
Colon cancer						
COLO 205	1.40	6.04	1.54	6.82	0.18	4.33
HCC-2998	1.47	–	1.51	5.68	0.26	21.68
HCT-116	1.42	6.16	1.29	5.38	0.08	54.58
HCT-15	1.19	5.21	1.39	5.52	6.46	100
HT29	1.65	–	1.27	–	0.12	67.45
KM12	1.76	–	1.73	6.09	0.27	92.68
SW-620	1.53	6.06	1.81	6.44	0.09	58.61
CNS cancer						
SF-268	1.80	–	1.74	7.19	0.10	30.48
SF-295	1.78	6.08	1.66	5.90	0.10	69.98
SF-539	1.62	5.91	1.58	5.72	0.12	27.23
SNB-19	1.89	–	1.75	5.86	0.04	49.77
SNB-75	1.63	5.92	1.54	5.50	0.07	3.30
U251	1.80	6.17	1.65	5.76	0.04	30.62
Melanoma						
LOX IMVI	1.44	–	1.51	–	0.07	50.35
MALME-3M	1.75	7.54	1.50	6.18	0.12	3.97
M14	1.68	6.01	1.58	6.19	0.18	4.05
MDA-MB-435	1.60	5.56	1.56	–	0.25	9.57
SK-MEL-2	2.11	7.13	1.84	–	0.17	1.06
SK-MEL-28	1.74	6.59	1.62	6.13	0.21	15.92
SK-MEL-5	1.56	5.78	1.38	5.28	0.08	0.49
UACC-257	2.09	9.04	1.95	7.14	0.14	8.15
UACC-62	1.87	6.25	1.82	5.80	0.12	0.74
Ovarian cancer						
IGROV1	1.82	7.02	1.65	6.44	0.17	100
OVCAR-3	1.81	–	1.66	5.91	0.39	84.33
OVCAR-4	1.60	–	1.45	–	0.37	74.30
OVCAR-5	1.59	6.06	1.51	5.52	0.41	100
OVCAR-8	2.27	–	1.83	6.73	0.10	43.25
NCI/ADR-RES	1.88	–	1.63	6.18	7.16	100
SK-OV-3	1.82	6.37	1.83	6.64	0.22	100
Renal cancer						
786-0	1.74	7.31	1.62	6.19	0.13	51.64
A498	1.50	5.70	2.17	3.30	0.10	1.90
ACHN	1.77	5.73	1.70	5.61	0.08	100
CAKI-1	1.66	5.51	1.55	5.40	0.95	100
RXF 393	1.75	6.95	1.68	6.04	0.10	4.69
SN12C	1.75	6.26	1.62	5.69	0.07	72.44
TK-10	1.86	6.67	1.76	6.96	–	–
UO-31	1.56	5.96	1.56	5.74	0.49	26.18
Prostate cancer						
PC-3	1.77	5.80	1.51	5.74	0.32	87.10
DU-145	1.59	5.55	1.63	5.58	0.11	100
Breast cancer						
MCF7	1.27	5.74	1.29	5.94	0.03	51.29
MDA-MB-31/ATCC	1.79	6.93	1.77	5.80	0.51	34.75
HS 578T	1.80	8.92	1.99	3.10	0.33	85.70
BT-549	1.70	–	1.79	–	0.23	21.33
T-47D	1.88	7.72	1.73	7.96	0.06	85.70
MDA-MB-468	1.75	7.08	1.66	6.88	0.05	2.52

[a]GI_{50} was the drug concentration resulting in a 50% reduction in the net protein increase (as measured by SRB staining) in control cells during the drug incubation, determined at five concentration levels (100, 10, 1.0, 0.1, and 0.01 μM)

[b]LC_{50} is a parameter of cytotoxicity and reflects the molar concentration needed to kill 50% of the cells

[c]Lopatina et al. (2019)

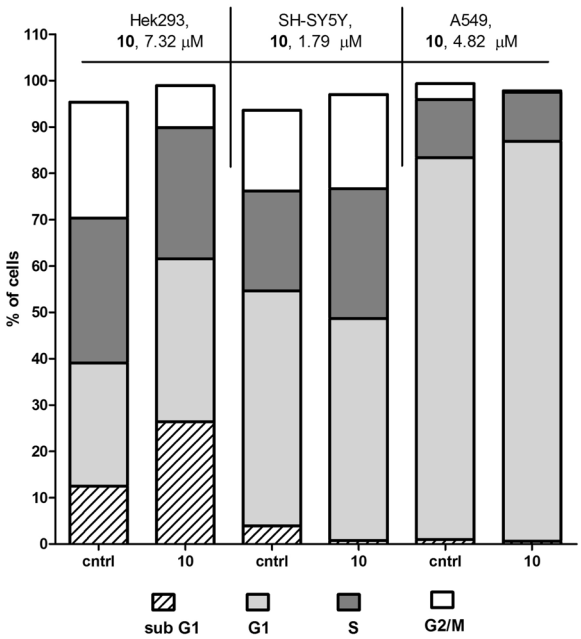

Fig. 2 Effect of compound **10** on cell cycle progression of non-cancerous and cancer cells. All values presented as mean ± SEM from two independent experiments, performed in triplicate

ESKAPE pathogens: five bacterial strains (gram-negative *Escherichia coli, Klebsiella pneumonia, Pseudomonas aeruginosa*, and *Acinetobacter baumannii* and gram-positive methicillin-resistant *S. aureus* (MRSA)). The

Table 3 % growth inhibition of compound **2**, **3**, **5**, **6**, and **10** at concentration 32 μg/mL

Compounds	Gram-positive bacteria	Gram-negative bacteria				Fungi	
	Staphylococcus Aureus	*Escherichia coli*	*Klebsiella pneumonia*	*Pseudomonas aeruginosa*	*Acinetobacter baumannii*	*Candida albicans*	*Cryptococcus neoformans* var. *grubii*
	Strain ATCC43300	Strain ATCC 25922	Strain ATCC 700603	Strain 19606	Strain ATCC 27853	Strain ATCC 90028	Strain H99, ATCC 208821
2	16.61	−5.37	1.30	3.45	21.32	14.67	0
3	19.50	−4.79	3.90	6.59	9.09	7.67	1.79
5	**97.51**	5.83	17.89	26.21	47.00	5.20	**95.91**
6	**93.90**	31.58	17.07	9.93	**73.64**	**100.90**	**99.23**
10	**99.76**	−0.25	7.50	23.35	20.01	8.38	**98.72**

Table 4 Antibacterial activity (MIC, μg/mL) for compounds **5**, **6**, and **10**

Comp.	Gram-positive bacteria	Gram-negative bacteria				Fungi	
	Staphylococcus Aureus	*Escherichia coli*	*Klebsiella pneumonia*	*Acinetobacter baumannii*	*Pseudomonas aeruginosa*	*Candida albicans*	*Cryptococcus neoformans* var. *grubii*
	Strain ATCC43300	Strain ATCC 25922	Strain ATCC 700603	Strain 19606	Strain ATCC 27853	Strain ATCC 90028	Strain H99, ATCC 208821
5	16	>32	>32	>32	>32	>32	>32
6	≤0.25	>32	>32	>32	>32	>32	>32
10	>32	>32	>32	>32	>32	>32	>32
Colistin	–	0.125	0.25	0.25	0.25	–	–
Vancomycin	1	–	–	–	–	–	–
Fluconazole	–	–	–	–	–	0.125	8

antifungal activity was determined against *C. albicans* and *C. neoformans*. Colistin and vancomycin were used as positive bacteria inhibitor standards for gram-negative and gram-positive bacteria, respectively. Fluconazole was used as a positive fungal inhibitor standard for *C. albicans* and *C. neoformans*.

In the primary screening the compounds **5**, **6**, and **10** showed antimicrobial activity against *S. aureus* bacteria cultures and culture of fungi *Cryptococcus neoformans var. grubii*. Compound **6** was also active against bacteria *Acinetobacter baumannii* and fungi *C. albicans* (Table 3).

For these compounds, a minimum inhibitory concentration was determined for the above cultures of bacteria and fungi. Compound **5** showed weak activity against MRSA (MIC = 16 μg/mL), while the compound **6** exhibited significant bacteriostatic effect against MRSA (MIC ≤ 0.25 μg/mL) that exceeds the effect of the clinically used antibiotic vancomycin (MIC = 1 μg/mL). Compound **10** did not show antibacterial activity after repeated screening (Table 4).

Conclusions

Starting from 3,28-dioximino-betulin we have synthesized a series of C28-amino-lupanes holding A-azepano- and A-seco-3-amino-fragments, their cytotoxicity toward the NCI-60 cancer cell line panel and antimicrobial activity against key ESKAPE pathogens were evaluated. A-azepano-28-amino-betulin exhibited remarkable activities with GI_{50} ranging from 1.16 to 2.27 μM against all panel with the highest activity toward leukemia, colon cancer, non-small cell lung cancer, and breast cancer. The replacement of the hydroxyl group at C28 in A-azepano-betulin to the amino group did not show a strong effect on the cytotoxic activity. Both compounds were ~5 and ~4 times more active than doxorubicin against colon cancer HCT-15 and ovarian cancer NCI/ADR-RES cell lines that make them promising structures for the future anticancer drug development. The ability of A-azepanobetulin to inhibit cell growth may be associated with its cytostatic effect, which, depending on the cell line, is associated with the arrest of either S or G1

phase of the cell cycle. 3-Amino-3,4-seco-28-amino-lup-4 (23),20(29)-dien exhibited significant bacteriostatic effect against MRSA (MIC ≤ 0.25 μg/mL) that exceeds the effect of the clinically used antibiotic vancomycin. The combination of cytotoxicity and antimicrobial activity in a series of A-azepano- and A-seco-3-amino-C28-aminolupanes makes them perspective scaffolds for further research.

Acknowledgements This work was supported by Federal programs (N AAAA-A20-120012090023-8, AAAA-A20-120012090029-0, and AAA A-A17-117011910028-7). The synthesis of compounds **2**, **4**, **5**, and **9-11** and evaluation of their biological activity were supported by the Russian Foundation for Basic Research (project no. 18-33-00364 for TVL). We thank National Cancer Institute for the screening of cytotoxicity of compounds **2**–**11**. The antimicrobial screening was performed by CO-ADD (The Community for Antimicrobial Drug Discovery) and funded by the Wellcome Trust (UK) and The University of Queensland (Australia).

Compliance with ethical standards

Conflict of interest The authors declare that they have no conflict of interest.

References

Ali-Seyed M, Jantan I, Vijayaraghavan K, Bukhari SNA (2016) Betulinic acid: recent advances in chemical modifications, effective delivery, and molecular mechanisms of a promising anticancer therapy. Chem Biol Drug Des 87(4):517–536. https://doi.org/10.1111/cbdd.12682

Bednarczyk-Cwynar B, Zaprutko L, Froelich A (2013) Beckmann rearrangement of oxime obtained from oleanolic acid. Structure elucidation of the initial oxime. J Mol Str 1053:115–121. https://doi.org/10.1016/j.molstruc.2013.09.006

Bildziukevich U, Özdemir Z, Wimmer Z (2019) Recent achievements in medicinal and supramolecular chemistry of betulinic acid and its derivatives. Molecules 24(19):3546. https://doi.org/10.3390/molecules24193546

Boyd MR, Paul KD (1995) Some practical considerations and applications of the National Cancer Institute in vitro anticancer drug discovery screen. Drug Res Rep. 34:91–109

Bruker (2014) APEX2 and SAINT. Bruker AXS Inc, Madison, WI

Catteau GL, Zhu L, Bambeke FV, Quetin-Leclercq J (2018) Natural and hemi-synthetic pentacyclic triterpenes as antimicrobials and resistance modifying agents against Staphylococcus aureus: a review. Phytochem Rev 17:1129–1163. https://doi.org/10.1007/s11101-018-9564-2

Chung PY (2019) Novel targets of pentacyclic triterpenoids in Staphylococcus aureus: a systematic review. Phytomedicine: 152933. https://doi.org/10.1016/j.phymed.2019.152933

Csuk R (2014) Betulinic acid and its derivatives: a patent review (2008–2013). Expert Opin Ther Pat 24:913–923. https://doi.org/10.1517/13543776.2014.927441

Flekhter OB, Ashavina OY, Boreko EI, Karachurina LT, Pavlova NI, Kabal'nova NN, Savinova OV, Galin FZ, Nikolaeva SN, Zarudii FS, Baltina LA, Tolstikov GA (2002) Synthesis of 3-O-acetylbetulinic and betulonic aldehydes according to Svern and the pharmacological activity of related oximes. Pharm Chem J 36:303–306. https://doi.org/10.1023/A:1020824506140

Grever MR, Schepartz SA, Chabner BA (1992) The National Cancer Institute: cancer drug discovery and development program. Semin Oncol 19:622–638

Giniyatullina GV, Kazakova OB, Baikova IP, Yamansarov EY, Osterman IA, Komarova ES, Skvortsov DA, Saltikova IV, Majouga AG, Ivanenkov YA (2019) Synthesis and cytotoxicity of *N*-methylpiperazinylamide azepanobetulinic acid. Nat Prod Comm 14:1–5. https://doi.org/10.1177/1934578X19860670

Giniyatullina GV, Mustafin AG, Kazakova OB (2020) Synthesis and antitumor activity of 3-amino-3,4-*Seco*-Lupa-4(23),20(29)-Diene Derivatives. Chem Nat Comp 1:84–88. https://doi.org/10.1007/s10600-020-02951-1

Hoz ADe la, Cortés JA (2019) Bacterial and atypical infections in critically Ill cancer patients. Oncol Crit Care: 379–1400. https://doi.org/10.1007/978-3-319-74588-6_123

Kazakova OB, Brunel JM, Khusnutdinova EF, Negrel S, Giniyatullina GV, Lopatina TV, Petrova AV (2019b) A-ring modified triterpenoids and their spermidine-aldimines with strong antibacterial activity. Molbank: M1078. https://doi.org/10.3390/M1078

Kazakova OB, Giniyatullina GV, Medvedeva NI, Lopatina TV, Baikova IP, Tolstikov GA, Apryshko GN (2014) Synthesis and cytotoxicity of triterpenoids seven members cyclic amines. Russ J Bioorg Chem 40:217–225. https://doi.org/10.1134/s106816201402006x

Kazakova OB, Rubanik LV, Smirnova IE, Savinova OV, Petrova AV, Poleschuk NN, Khusnutdinova EF, Boreko EI, Kapustsina YM (2019a) Synthesis and in vitro activity of oleanane type derivatives against *Chlamydia trachomatis*. Org Commun 12:169–175. https://doi.org/10.25135/acg.oc.66.19.07.1352

Khusnutdinova EF, Petrova AV, Thi Thu HN, Thi Tu AL, Thanh TN, Ba Thi C, Babkov DA, Kazakova OB (2019) Structural modifications of 2,3-indolobetulinic acid: design and synthesis of highly potent α-glucosidase inhibitors. Bioorg Chem 88:102957. https://doi.org/10.1016/j.bioorg.2019.102957

Khusnutdinova EF, Smirnova IE, Giniyatullina GV, Medvedeva NI, Yamansarov EY, Kazakov DV, Kazakova OB, Linh PT, Viet Q, Huong DT (2016) Inhibition of alpha-glucosidase by synthetic derivatives of lupane, oleanane, ursane and dammarane triterpenoids. Nat Prod Comm 11:33–35. https://doi.org/10.1177/1934578X1601100112

Krasutsky PA (2006) Birch bark research and development. Nat Prod Rep. 23:919–942

Kumar S, Misra N, Raj K, Srivastava K, Puri SK (2008) Novel class of hybrid natural products derived from lupeol as antimalarial agents. Nat Prod Res 22(4):305–319. https://doi.org/10.1080/14786410701766349

Lopatina TV, Medvedeva NI, Baikova IP, Iskhakov AS, Kazakova OB (2019) Synthesis and cytotoxicity of *O*- and *N*-acyl derivatives of azepanobetulin. Russ J Bioorg Chem 45:292–301. https://doi.org/10.1134/S106816201904006X

Medvedeva NI, Kazakova OB, Lopatina TV, Smirnova IE, Giniyatullina GV, Baikova IP, Kataev VE (2018) Synthesis and antimycobacterial activity of triterpenic A-ring azepanes. Eur J Med Chem 143:464–472. https://doi.org/10.1016/j.ejmech.2017.11.035

Monks A, Scudiero DA, Johnson GS, Paull KD, Sausville EA (1997) The NCI anti-cancer drug screen: a smart screen to identify effectors of novel targets. Anticancer Drug Des 12:533–541

Monks A, Scudiero D, Skehan P, Shoemaker R, Paull KD, Vistica D, Hose C, Langley J, Cronise P, Vaigro-Wolff A, Gray-Goodrich M, Campbell H, Mayo J, Boyd MJ (1991) Feasibility of a highflux anticancer drug screen using a diverse panel of cultured human tumor cell lines. Nat Cancer Inst 183:757–766

Montoya A, Quiroga J, Abonia R, Nogueras M, Cobo J, Insuasty B (2014) Synthesis and in vitro antitumor activity of a novel series of 2-pyrazoline derivatives bearing the 4-aryloxy-7-chloroquinoline fragment. Molecules 19:18656–18675. https://doi.org/10.3390/molecules191118656

Sheldrick GM (2015) Crystal structure refinement with SHELXL. Acta Crystallogr C71:3–8

Smirnova IE, Petrova AV, Kazakova OB (2019) Synthesis and cytotoxicity of A-azepanodammaradiene. Chem Nat Compd 55:883–889. https://doi.org/10.1007/s10600-019-02838-w

Sousa JLC, Freire CSR, Silvestre AJD, Silva AMS (2019) Recent developments in the functionalization of betulinic acid and its natural analogues: a route to new bioactive compounds. Molecules 24(2):355. https://doi.org/10.3390/molecules24020355

Tolmacheva IA, Nazarov AV, Eroshenko DV, Grishko VV (2018) Synthesis, cytotoxic evaluation, and molecular docking studies of the semi-synthetic "triterpenoid-steroid" hybrids. Steroids 140:131–143. https://doi.org/10.1016/j.steroids.2018.10.005

Tolstikov GA, Flekhter OB, Shul'ts EE, Baltina LA, Tolstikov AG (2005) Betulin and its derivatives. Chemistry and biological activity. Khim Interes Ustoich Razvit 13:1–30

Tolstikova TG, Sorokina IV, Tolstikov GA, Tolstikov AG, Flekhter OB (2006) Biological activity and pharmacological prospects of lupane terpenoids: I. natural lupane derivatives. Russ J Bioorg Chem 32:37–49. https://doi.org/10.1134/S1068162006010031

Weinstein JN, Myers TG, O'Connor PM, Friend Jr. SH, Fornace AJ, Kohn KW, Fojo T, Bates SE, Rubinstein LV, Anderson NL, Buolamwini JK, van Osdol WW, Monks AP, Scudiero DA, Sausville EA, Zaharevitz DW, Bunow B, Viswanadhan VN, Johnson GS, Wittes RE, Paull KD (1997) An information-intensive approach to the molecular pharmacology of cancer. Science 275:343–349. https://doi.org/10.1126/science.275.5298.343

Yli-Kauhaluoma J, Alakurtti S, Minkkinen J, Sarcerdoti-Sierra N, Jaffe CL, Heiska T (2010) Betulin derived compounds useful as antiprotozoal agents. US Patent 2010190795, filled 6 June 2007, issued 28 Oct 2010

Zhang DM, Xu HG, Wang L, Li YJ, Sun PH, Wu XM, Wang GJ, Chen WM, Ye WC (2015) Betulinic acid and its derivatives as potential antitumor agents. Med Res Rev 35:1127–1155. https://doi.org/10.1002/med.21353